



ELSEVIER

Earth and Planetary Science Letters 160 (1998) 695–707

EPSL

Climate change during the last 150 million years: reconstruction from a carbon cycle model

Eiichi Tajika*

Geological Institute, School of Science, University of Tokyo, 7-3-1 Hongo, Bunkyo-ku, Tokyo 113, Japan

Received 17 December 1997; revised version received 29 May 1998; accepted 31 May 1998

Abstract

Variations of the atmospheric CO₂ level and the global mean surface temperature during the last 150 Ma are reconstructed by using a carbon cycle model with high-resolution input data. In this model, the organic carbon budget and the CO₂ degassing from the mantle, both of which would characterize the carbon cycle during the Cretaceous, are considered, and the silicate weathering process is formulated consistently with an abrupt increase in the marine strontium isotope record for the last 40 Ma. The second-order variations of the atmospheric CO₂ level and the global mean surface temperature in addition to the first-order cooling trend are obtained by using high-resolution data of carbon isotopic composition of marine limestone, seafloor spreading rate, and production rate of oceanic plateau basalt. The results obtained from this model are in good agreement with the previous estimates of palaeo-CO₂ level and palaeoclimate inferred from geological, biogeochemical, and palaeontological models and records. The system analyses of the carbon cycle model to understand the cause of the climate change show that the dominant controlling factors for the first-order cooling trend of climate change during the last 150 Ma are tectonic forcing such as decrease in volcanic activity and the formation and uplift of the Himalayas and the Tibetan Plateau, and, to a lesser extent, biological forcing such as the increase in the soil biological activity. The mid-Cretaceous was very warm because of the high CO₂ level (4–5 PAL) maintained by the enhanced CO₂ degassing rate due to the increased mantle plume activities and seafloor spreading rates at that time, although the enhanced organic carbon burial would have a tendency to decrease the CO₂ level effectively at that period. The variation of organic carbon burial rate may have been responsible for the second-order climate change during the last 150 Ma. © 1998 Elsevier Science B.V. All rights reserved.

Keywords: atmosphere; carbon; cycles; paleoclimatology; mantle; degassing; silicates; weathering; organic carbon; burial; Cretaceous; climate

1. Introduction

Climate change on a geological timescale is now believed to be caused mainly by atmospheric CO₂ variations (e.g., [1–7]). According to the recent studies on the geochemical cycle of carbon, the abun-

dance of atmospheric CO₂ on the timescale of >10⁶ years is regulated by the carbon cycle which includes geological processes such as silicate weathering, carbonate precipitation, carbonate metamorphism, mantle CO₂ degassing, oxidative weathering and burial of organic carbon, and so on [3–14]. Variations of atmospheric CO₂ level predicted by carbon cycle models are roughly consistent with the climate change inferred from the geological record during

* Tel.: +81 (3) 3812-2111 ext.4516; Fax: +81 (3) 3815-9490; E-mail: tajika@geol.s.u-tokyo.ac.jp

both the past 100 Ma [3,4,9,15,16] and the Phanerozoic [5–7]. This indicates a significant role of the carbon cycle on the long-term climate change.

The middle to Late Cretaceous is known to have been one of the warmest periods during the Phanerozoic: the average global temperature was probably $>6^{\circ}\text{C}$ higher than that of today, there is no evidence of permanent and seasonal ice, forests and vertebrates occurred near both poles, and warm anoxic oceans may have promoted organic carbon burial (e.g., [1,17]). Because the global seafloor spreading rate was almost twice the present one (e.g., [18,19]), and also because large amounts of oceanic plateau basalt were produced at that time [19], high atmospheric CO_2 levels might have been maintained as a result of an effective metamorphism–volcanism of carbonates in addition to the small land area [3,4,15] and an effective CO_2 degassing from the mantle [11] at that time. Decreasing mantle activities and the formation and uplift of the Himalayas and the Tibetan Plateau may have been responsible for the Mesozoic–Cenozoic cooling trend (e.g., [3–6,20]). Because there are large quantities of geological, geochemical, and geophysical data which are much more reliable and have higher resolution for the past 100–150 Ma than those for older ages, application and interpretation of geochemical cycle models to the climate change during this period will be preferable.

The earliest general models of geochemical cycles (known as the BLAG-type model) were applied to study the climate change during the last 100 Ma, and predicted a high CO_2 level and thus a warm climate at the mid-Cretaceous [3,4,9,15,16]. More simplified models of carbon cycle (known as the GEOCARB-type model), specialized to estimate the atmospheric CO_2 variations, were applied to study the climate change during the Phanerozoic, and also predicted the warm Cretaceous [5–7]. All these models have shown a general cooling trend, that is, the first-order variation of atmospheric CO_2 during the last 100 Ma. However, although the mantle activity and the organic carbon burial may have been intense and thus essential to the carbon cycle during the Cretaceous, there was no previous model which took into account the influences of both (1) the distinction of mantle CO_2 degassing due to mid-ocean ridge volcanism and hot spot volcanism from the metamorphic CO_2 degassing at subduction zones, and (2)

variations of organic carbon budget, by using (3) high-resolution input data for the carbon cycle system. As a result, none of the previous studies could discuss the relative contributions of mantle degassing and organic carbon burial, which may characterize the carbon cycle during the Cretaceous, to the variations of the atmospheric CO_2 level and the climate, especially for their second-order variations, during the last 100–150 Ma.

In this paper, the second-order variations of atmospheric CO_2 and climate change during the past 150 Ma are reconstructed by using the carbon cycle model with high-resolution input data of the carbon isotope record of marine carbonates, seafloor spreading rate, and production rate of oceanic plateau basalt. Results of the analyses for the carbon cycle model to understand the causes of the climate change during this period will be discussed.

2. Models

The carbon cycle model considered in this study is shown in Fig. 1. Because the main purpose of this study is concentrated on estimating variations of atmospheric CO_2 level and the global mean surface temperature (i.e., the climate) during the last 150 Ma, a simple GEOCARB-type model is adopted here. Although the model is based on the GEOCARB II [6], several modifications are made as described below. It is essential for this model to include processes of CO_2 degassing from the mantle due both to mid-ocean ridge volcanism and to hot spot volcanism (mainly producing a large quantity of oceanic plateau basalts) explicitly to estimate influences of mantle activity on the carbon cycle and the climate during the mid-Cretaceous (Fig. 1). Although Caldeira and Rampino [11] constructed such a model, they did not consider the organic carbon budget which would have been another essential factor to the carbon cycle during the Cretaceous. Furthermore, they simply assumed that the whole CO_2 degassing flux is due to the processes of oceanic crustal production. In this study, the flux of CO_2 degassing is divided into four processes (Fig. 1): degassing of CO_2 due to (1) mid-ocean ridge volcanism, (2) hot spot volcanism, (3) metamorphism of carbonate at subduction zones, and (4) metamorphism of organic carbon at subduc-

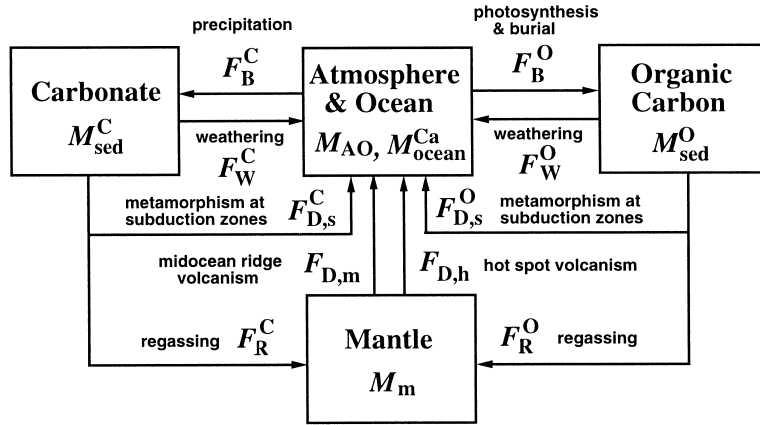


Fig. 1. The carbon cycle model considered in this study. Boxes and arrows represent chemical reservoirs and fluxes. See text for symbols and fluxes expressions.

tion zones. These four processes are distinguished in this study because we need to know the influence of each type of degassing for the climate, especially during the Cretaceous, and also because we use these fluxes to calculate the carbon isotope budget within the system as will be described later. It is noted that the previous models (e.g., [3–7,9,11]) did not distinguish each type of degassing, but the global sum of all degassing rates should be essentially a similar value because all these models assume the present-day steady state of the carbon cycle system.

The model also includes the regassing processes of carbonate carbon and organic carbon into the mantle by subduction of oceanic plates into the mantle (Fig. 1). Regassing of carbon into the mantle has been inferred from the observed carbon budget at subduction zones (e.g., [21–23]). Regassing processes are considered here just because we assume a steady state of the carbon cycle system at present. Although the regassing of carbon into the mantle might have been important for the carbon cycle on a timescale of >1 Ga [12–14], the total amounts of subducted carbon during 150 Ma may be small (<several %) compared with abundance of the total crustal carbon.

Mass balance equations used in this study are as follows:

$$\frac{dM_{AO}}{dt} = F_{D,m} + F_{D,h} + F_{D,s}^C + F_{D,s}^O + F_W^C + F_W^O - F_B^C - F_B^O = 0 \quad (1)$$

$$\frac{dM_{sed}^C}{dt} = F_B^C - F_W^C - F_{D,s}^C - F_R^C \quad (2)$$

$$\frac{dM_{sed}^O}{dt} = F_B^O - F_W^O - F_{D,s}^O - F_R^O \quad (3)$$

$$\frac{dM_{ocean}^{Ca}}{dt} = F_W^S + F_W^C - F_B^C = 0 \quad (4)$$

where M_{AO} is amount of carbon in the atmosphere–ocean system, M_{sed} is amount of carbon in the crustal sediments, M_{ocean}^{Ca} is amount of calcium ion in the ocean, $F_{D,m}$ is degassing rate of CO_2 due to midocean ridge volcanism, $F_{D,h}$ is degassing rate of CO_2 due to hot spot volcanism, $F_{D,s}$ is degassing rate of CO_2 due to metamorphism–volcanism at subduction zones, F_W is weathering rate, F_B is burial rate, and F_R is regassing rate. Superscripts C, O, and S represent carbonate carbon, organic carbon, and silicate, respectively. Carbon in the atmosphere–ocean system (M_{AO}) is assumed to be in a steady state because the residence time of this quantity is short ($<10^6$ years) compared with the timescale considered in this study (e.g., [5,6,9,15]). For simplicity, all carbonate carbon is regarded as the form of calcite, and calcium is considered as the only cation in relation to the carbon cycle (e.g., [5,6]). Calcium is assumed to be carried into the ocean by weathering of silicates and carbonates, and to be precipitated as seafloor carbonates. The amount of calcium ion in the ocean (M_{ocean}^{Ca}) is also assumed to be in a steady state, that

is, the same amount of calcium supplied to the ocean is assumed to be precipitated as carbonates.

Isotope mass balance equations used in this study are as follows:

$$\begin{aligned} \frac{d\delta_{AO}M_{AO}}{dt} &= \delta_M(F_{D,m} + F_{D,h}) + \delta_{sed}^C(F_{D,s}^C + F_W^C) \\ &\times \delta_{sed}^O(F_{D,s}^O + F_W^O) - \delta_{AO}F_B^C - (\delta_{AO} - \Delta)F_B^O \\ &= 0 \end{aligned} \quad (5)$$

$$\frac{d\delta_{sed}^C M_{sed}^C}{dt} = \delta_{AO}F_B^C - \delta_{sed}^C(F_W^C + F_{D,s}^C + F_R^C) \quad (6)$$

$$\frac{d\delta_{sed}^O M_{sed}^O}{dt} = (\delta_{AO} - \Delta)F_B^O - \delta_{sed}^O(F_W^O + F_{D,s}^O + F_R^O) \quad (7)$$

where δ represents $\delta^{13}C$ value ($= [(^{13}C/^{12}C)_{sample}/(^{13}C/^{12}C)_{standard} - 1] \times 1000\text{‰}$) and Δ represents the carbon isotope fractionation factor through the photosynthetic process. Subscripts AO and M represent the atmosphere–ocean system and the mantle, respectively. Because of the same reason for the amount of carbon in the atmosphere–ocean system, the amount of carbon isotope in the atmosphere–ocean system ($\delta_{AO}M_{AO}$) is also assumed to be in a steady state (e.g., [5,6]). In these equations, carbon isotope of marine carbonates δ_{AO} and carbon isotope fractionation factor Δ are used as input data in the model.

Mass fluxes in the above equations are expressed as follows:

$$F_{D,m}(t) = f_{SR}(t)F_{D,m}^* \quad (8)$$

$$F_{D,h}(t) = f_h(t)F_{D,h}^* \quad (9)$$

$$F_{D,s}^C(t) = k_{D,s}^C f_{SR}(t) f_C(t) M_{sed}^C \quad (10)$$

$$F_{D,s}^O(t) = k_{D,s}^O f_{SR}(t) M_{sed}^O \quad (11)$$

$$F_R^C(t) = k_R^C f_{SR}(t) f_C(t) M_{sed}^C \quad (12)$$

$$F_R^O(t) = k_R^O f_{SR}(t) M_{sed}^O \quad (13)$$

$$F_W^C(t) = k_W^C f_{BB}(t) f_{LA}(t) f_E(t) f_D(t) M_{sed}^C \quad (14)$$

$$F_W^O(t) = k_W^O f_D(t) M_{sed}^O \quad (15)$$

Table 1

Constants used in the model

Parameter	Value	Notes and references
$F_{D,m}^*$	2×10^{18} mol/Ma	[29]
$F_{D,h}^*$	0.17×10^{18} mol/Ma	(see text)
F_W^{S*}	6.7×10^{18} mol/Ma	[5,6]
k_W^C	0.0026 Ma ⁻¹	[5,6]
k_W^O	0.0030 mol/Ma	[5,6]
$k_{D,s}^C$	1.0468×10^{-3} Ma ⁻¹	(see text)
$k_{D,s}^O$	4.3664×10^{-4} Ma ⁻¹	(see text)
k_R^C	2.9316×10^{-4} Ma ⁻¹	(see text)
k_R^O	5.6336×10^{-4} Ma ⁻¹	(see text)
$M_{sed}^C(0)$	5000×10^{18} mol	[44]
$M_{sed}^O(0)$	1250×10^{18} mol	[44]
$\delta_{AO}(0)$	1.0‰	[44]
$\Delta(0)$	21.8‰	[5,6]
$\delta_{sed}^C(0)$	1.5‰	[44]
$\delta_{sed}^O(0)$	-23.5‰	[44]
$\delta_M(t)$	-5.0‰	[45]

where f_{SR} is the seafloor spreading rate, f_h is the production rate of oceanic plateau basalt, f_C is the precipitation factor (relative proportions of carbonates in the shallow water and in the deep sea), f_E is the soil biological activity factor, f_D is the river runoff factor due to changes in palaeogeography, f_{LA} is the carbonate land area factor, f_{BB} is the feedback function for carbonate weathering. Superscript asterisk represents the present value. All these functions are normalized to the present values (i.e., f_i is 1 at present). Because $F_{D,s}$ and F_R must be related to the carbon mass, these fluxes depend on M_{sed} . Data for functions $f_i(t)$ and coefficients k_i are basically the same as those used in GEOCARB II [6], although some of them are changed by assuming the condition of steady state of the system at present (Table 1). It is noted that the soil biological activity factor (f_E) may have increased from about 0.75 to 1.0 between 130 Ma and 80 Ma because of the advent and diversification of angiosperm–deciduous ecosystems, which will affect the global weathering rate after that period [5,6,24].

Then, we consider the formulation of the silicate weathering rate. Berner [6] presented the following formulation:

$$F_W^S(t) = f_B(t) f_R(t) f_E(t) f_D(t)^{0.65} F_W^{S*} \quad (16)$$

where f_B is a feedback function for silicate weathering rate and f_R is an uplift factor. In this formulation, there may be some difficulties in defining the uplift factor f_R . The formation and uplift of the Himalayas and the Tibetan Plateau (hereafter referred to as HTP) have resulted in an abrupt increase in erosion rate and chemical weathering rate during the last 40 Ma, which is also suggested from increase in the strontium isotope record during this period (e.g., [20,25–27]). Berner [6] thus modeled this effect by using strontium isotope data as $f_R = 1 - L[(R_{ocb} - R_{ocm})/(R_{ocb} - 0.7)]$, where L is the uplift proportionality (a free parameter), R_{ocm} is the actual $^{87}\text{Sr}/^{86}\text{Sr}$ value recorded in marine carbonates, and R_{ocb} is the calculated $^{87}\text{Sr}/^{86}\text{Sr}$ value from the model considering the basalt–seawater reaction process only (see [6]). However, this may not be an appropriate expression for this factor as Berner himself noted [6]. This is because, for example, observed $^{87}\text{Sr}/^{86}\text{Sr}$ increase during the last 40 Ma is probably due not to the enhanced global weathering rate but rather to the extraordinary high $^{87}\text{Sr}/^{86}\text{Sr}$ value provided from the HTP (e.g., [26,27]). Therefore, we had better develop another formulation for the silicate weathering process which may be consistent with the Sr isotope record. In this study, we use the following expression:

$$F_w^S(t) = F_{W,Global}^S(t) + F_{W,HTP}^S(t)[(1 - \beta) \times f_B(t)f_E(t)f_D(t)^{0.65} + \beta f_R(t)]F_w^{S*} \quad (17)$$

where $F_{W,Global}^S$ and $F_{W,HTP}^S$ represent the remaining global chemical weathering rate and the weathering rate for the HTP due to the formation and uplift of this region, respectively. The uplift factor $f_R(t)$ is assumed to affect $F_{W,HTP}^S$ through the effective erosion of the HTP for the last 40 Ma. We adopt the erosion rate for the HTP estimated by Richter et al. [26] as the uplift factor, which is obtained so as to be consistent with the marine strontium isotope record (fig. 8 in [26]; normalized to the present-day value and assumed to be zero before 50 Ma). We assume that climate change has a negligible effect on the weathering rate for the HTP region, and that the chemical weathering of this region before 50 Ma is negligibly small (because the HTP region makes up only 4% of the Earth's land surface). It is noted that there seems to be no other mountain building so large

as the HTP during the last 150 Ma. The β is a free parameter which represents the contribution of the Ca dissolution from the HTP region and the eroded HTP materials into the ocean to the worldwide total supply of Ca due to the global chemical weathering. This expression is used in this study because it may be more reasonable than that presented by Berner [6] to express the effect of the HTP uplift and its erosion on the global weathering rate, and also because this may be formulated consistently with Sr isotope variations for the last 50 Ma (see also [26]).

The feedback function f_B , which represents the dependence of the weathering rate on the CO_2 partial pressure and the temperature, is a critical factor to estimate the atmospheric CO_2 level and the surface temperature in the carbon cycle model (e.g., [3–9,11]). This factor may be expressed by multiplying the river runoff and the river bicarbonate ion concentration (e.g., [3–6,8,9,11]). Three types of expression for this factor, considering the dissolution kinetics of silicate and the CO_2 fertilization due to land plants and microbes, are used in this study.

Walker et al. [8] presented the expression for the feedback function derived from the dissolution kinetics of silicate and the possible enhancement of global precipitation due to elevated global temperature as follows:

$$f_B = \left(\frac{P_{\text{atm}}}{P_{\text{atm}}^*}\right)^{0.3} \exp\left(\frac{\Delta T}{13.7}\right) \quad (18)$$

where P_{atm} is atmospheric CO_2 partial pressure and ΔT represents the temperature difference from the present value. This was the first proposal for the global weathering process to work as a negative feedback mechanism for the atmospheric CO_2 level and the surface temperature.

It is known that the CO_2 pressure in soils is 10–100 times higher than the atmospheric CO_2 partial pressure due to respiration of plant roots and microbes. Volk [9] modified the formulation presented by Walker et al. [8] to include the influence of enhanced CO_2 level in the soil as follows:

$$f_B = \left(\frac{P_{\text{soil}}}{P_{\text{soil}}^*}\right)^{0.3} \exp\left(\frac{\Delta T}{13.7}\right) \quad (19)$$

$$\frac{P_{\text{soil}}}{P_{\text{soil}}^*} = \frac{\Pi}{\Pi^*} \left(1 - \frac{P_{\text{atm}}^*}{P_{\text{soil}}^*}\right) + \frac{P_{\text{atm}}}{P_{\text{soil}}^*} \quad (20)$$

$$\Pi = \Pi_{\max} \frac{P_{\text{atm}} - P_{\min}}{P_{1/2} + (P_{\text{atm}} - P_{\min})} \quad (21)$$

where P_{soil} is the soil CO_2 pressure, Π is the total soil biological productivity, Π_{\max} is the maximum productivity, $P_{1/2}$ is the value at which $\Pi = 0.5\Pi_{\max}$, and P_{\min} is the value of P_{atm} at which the rate of carbon fixation just balances the photorespiration [9]. Eq. 21 represents the Michaelis–Menton equation which is generally useful in describing the effects of CO_2 on plant growth [9]. Following Volk [9], we assume $P_{\text{soil}}^* = 10P_{\text{atm}}^*$, $P_{\min} = 0.2P_{\text{atm}}^*$, and $\Pi_{\max} = 2\Pi^*$.

Berner [6] presented a similar feedback function in the GEOCARB model, which is expressed as follows:

$$f_B = \left(\frac{2P_{\text{atm}}/P_{\text{atm}}^*}{1 + P_{\text{atm}}/P_{\text{atm}}^*} \right)^{0.4} (1 + 0.038\Delta T)^{0.65} \times \exp(0.090\Delta T) \quad (22)$$

In this study, this expression is adopted as a standard, although the results derived from other two types of feedback function will be compared. For the feedback function of the carbonate weathering (f_{BB}), the expression presented by Berner [6] is adopted in this study.

Larson [19] estimated the temporal variations of production rates of the mid-oceanic ridge basalt and the oceanic plateau basalt during the last 150 Ma (Fig. 2), which are based on the detailed analyses of mid-oceanic ridge length, seafloor spreading rate, oceanic plateau volumes, and so on. Although the large seafloor spreading rate during the Cretaceous

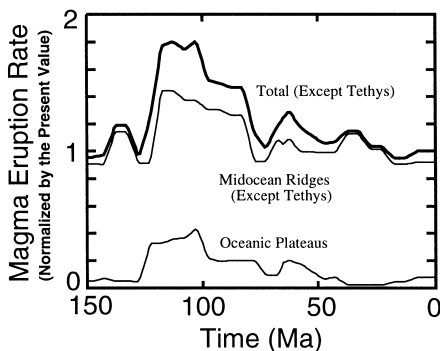


Fig. 2. Magma production rates for the mid-ocean ridge basalt and the oceanic plateau basalt during the last 150 Ma (after Ref. [19]).

proposed by Larson is questioned recently (e.g., [46]), the result of Larson [19] can be regarded, at least, as an upper estimate for the crustal production rate during the Cretaceous. The results of Larson are used as input data (f_{SR} and f_{h}) to estimate degassing fluxes of CO_2 at mid-ocean ridges and at hot spots. The factor f_{SR} can be regarded as the seafloor spreading rate when we assume that the thickness of oceanic crust has been constant through the time. Therefore it is also used to estimate the CO_2 degassing rate at subduction zones due to metamorphism of carbonates and organic carbon. The present-day CO_2 degassing rate at mid-ocean ridges is estimated to be $(1-8) \times 10^{18}$ mol/Ma (e.g., [21,23,28–30]). Among these, the estimate of 2×10^{18} mol/Ma by Marty and Jambon [29] is adopted here because larger estimates are not consistent with the silicate weathering rate of 6.7×10^{18} mol/Ma [6], which should be roughly equal to $F_{\text{D,m}} + F_{\text{D,h}} + F_{\text{D,s}}^{\text{C}}$ in a steady-state system (see Eqs. 1–4 and Fig. 1). If we assume the same carbon content in magma sources (e.g., [11]), the CO_2 degassing rate due to hot spot volcanism at present is 0.17×10^{18} mol/Ma, which is $\sim 1/10$ of the mid-ocean CO_2 degassing rate. It is noted that the CO_2 degassing inferred from oceanic plateau basalt production is $\sim 1/4$ of the degassing at the mid-oceanic ridges during the mid-Cretaceous. The metamorphic CO_2 degassing rates are determined by the constraints of the carbon mass balance and the carbon isotope mass balance, assuming a steady state in the present-day carbon cycle system.

Data of carbon isotopic composition of pelagic marine limestone for the last 150 Ma are shown in Fig. 3. These data are compiled and modified from Arthur et al. [31] for the Cretaceous, and from Shackleton and Hall [32] and Shackleton [33] for the Cenozoic. In addition to this, the carbon isotope fractionation factor is also necessary for the model to estimate burial fluxes of carbon. Arthur et al. [34] pointed out that marine photosynthesis in the mid-Cretaceous and earlier oceans generally resulted in a greater fractionation of carbon isotopes and produced organic carbon having lighter $\delta^{13}\text{C}$ values. They concluded that modern marine photosynthesis may be occurring under unusual geological conditions such as higher oceanic primary production rate and the lower CO_2 partial pressure which limit dis-

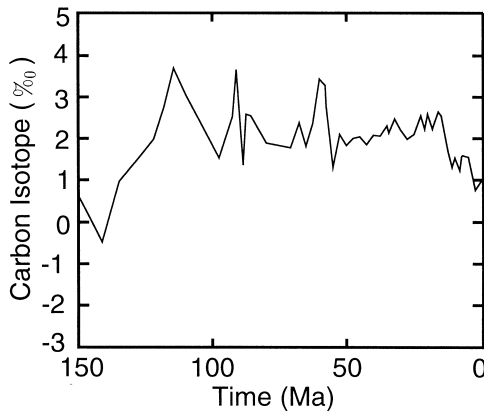


Fig. 3. Carbon isotope data of marine limestone during the last 150 Ma. Data are compiled and modified from Arthur et al. [34] for the Cretaceous, and from Shackleton and Hall [32] and Shackleton [33] for the Cenozoic.

solved CO_2 availability and minimize carbon isotope fractionation. Although a precise estimate of secular variation of the isotope fractionation factor throughout the last 150 Ma has not been obtained, a decrease in this factor seems to have been occurred effectively during the last 40 Ma (e.g., [35]; Ohkouchi, unpublished data). Then, the fractionation factor Δ is set to be 25‰ before 40 Ma and 21.8‰ at present, and we linear-interpolated them between 40 Ma and 0 Ma.

In order to estimate the global mean surface temperature by the greenhouse effect of atmospheric CO_2 and H_2O , the formulation of Caldeira and Kasting [36], which was proposed by compiling the results of 143 runs of one-dimensional radiative-convective climate models and was least-squares fitted with mean errors of $T < 0.5$ K, is used in this study.

Calculations are performed by using a backward differential scheme, that is, variables are time-integrated from the present time to the past to avoid the ambiguity of initial conditions of the model. The results are also checked by a forward differential scheme to verify the results of a backward scheme.

3. Numerical results

The results of temporal variations of the atmospheric CO_2 level and the global surface temperature during the last 150 Ma for the standard case are

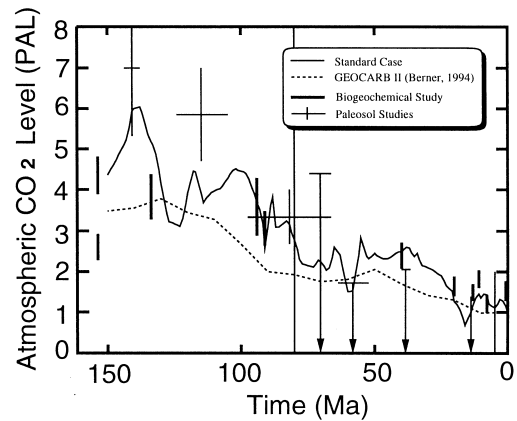


Fig. 4. The result of the temporal variation of CO_2 level (PAL = present atmospheric level) for the standard case. The result of GEOCARB II [6] is also shown for comparison. Vertical bars are the estimates of the palaeo- CO_2 level based on biogeochemical study [35] and vertical thin lines are the estimates of the palaeo- CO_2 level based on the studies of palaeosols (references are shown in Ref. [7]).

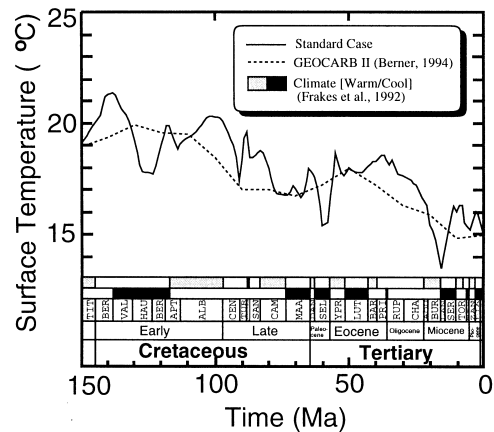


Fig. 5. The result of the temporal variation of the global mean surface temperature for the standard case. The result of GEOCARB II [6] is also shown for comparison (note that the way to estimate the greenhouse effect is different from this study). Palaeoclimates (warm/cool) as indicated in the geological record are also shown [1].

shown in Figs. 4 and 5. As shown in Fig. 4, the atmospheric CO_2 variation has a long-term decreasing trend with many short-term fluctuations. The long-term trend of decreasing CO_2 (hence the surface temperature) is consistent with the warm Cretaceous and the cool Cenozoic, although this trend itself was also reproduced by previous studies of carbon cycle

(e.g., [3–6,9,15]). Figs. 4 and 5 also show the results of one of these previous studies (GEOCARB II; [6]) for comparison. As shown in these figures, the results of this study are much higher resolved than the previous ones, and show the second-order variations in addition to the first-order cooling trend.

Fig. 4 also shows the estimates of palaeo-CO₂ levels based on the biogeochemical study by Freeman and Hays [35]. They estimated CO₂ partial pressures for several samples during the last 154 Ma from (1) a correlation between the fractionation of carbon isotope during photosynthetic fixation of CO₂ and concentrations of dissolved CO₂, (2) carbon isotope fractionations from analyses of sedimentary porphyrins, (3) chemical and isotopic equilibria in the dissolved inorganic carbon system and of air–sea equilibria, and (4) palaeotemperatures estimated from reconstructions of palaeogeography, latitudinal temperature gradients, and low-latitude sea surface temperature. In addition to these estimates, the inferred palaeo-CO₂ levels based on the studies of palaeosols (references are found in [7]) are also shown in Fig. 4 for comparison.

The average level of palaeo-CO₂ variation depends on β (the contribution of dissolution of Ca from the HTP region and the eroded HTP materials into the ocean to the worldwide total supply of Ca due to chemical weathering), that is, β is estimated so that the CO₂ levels may be consistent with the estimates of the palaeo-CO₂ levels. In the standard case, the estimated value of β is 0.45, which seems to be somewhat large, since the contribution of strontium carried by rivers through the HTP at present is estimated to be, at least, ~ 0.25 (this may not include the amount of Sr dissolved from the eroded materials within the ocean; see [26]). However, a smaller value of β (0.25–0.35) is obtained when the feedback function by Volk [9] is adopted in the model as will be shown later.

The short-term variations of the CO₂ level result in the short-term climate change during the past 150 Ma. Fig. 5 also shows the inferred climate (warm/cool) in each age suggested from the geological record such as oxygen isotope data, various fossil floras and faunas, and sedimentary facies [1]. For example, extensive ice-rafted deposits at high latitudes indicate the Valanginian and Hauterivian to have been quite cool. Oxygen isotope data and vegetation

of high latitudes indicate that the Albian was the warmest period, although the Coniacian and Campanian were also warm. During the Maastrichtian, freezing conditions may have prevailed in the northern polar region. Then, the climate warmed during the Early Paleocene, cooled during the Late Paleocene, and warmed again during the early Eocene. During the Tertiary, the climate change has step-like cooling phases, which were superimposed on the general cooling trend, probably due to the specific events mainly in tectonic origin and resulting in changing ocean circulation patterns [1]. In the Middle Miocene (13–15 Ma), the intensification of polar glaciation has been recorded by synchronous drops in both benthic and planktonic oxygen isotopes, suggesting a major cooling episode, which may be correlated with carbon isotope excursion [1]. As shown in Fig. 5, the result of the variations of surface temperature is roughly consistent with the pattern of palaeoclimate change described above. This suggests that climate change on a geological timescale is caused mainly by variations of the atmospheric CO₂ level, and variation of CO₂ is regulated mainly by the processes considered in this study. The CO₂ level at the mid-Cretaceous is estimated to be about 4–5 PAL (= present atmospheric level), corresponding to a surface temperature of about 20–21°C. The global mean surface temperature during the mid-Cretaceous has been estimated to be 6–14°C warmer than today [17], although it may have been much cooler than previously believed (e.g., [37]). Therefore, the result of this study is consistent with, at least, the lower estimate of palaeotemperatures at that time. It is noted that palaeogeographic factors (topography, continental positions, and sea level) could also increase global mean surface temperature with $\sim 4.8^\circ\text{C}$ [38]. Therefore the temperature increase of $\sim 10^\circ\text{C}$ might be possible.

There appear to be, however, some phase lags between the numerical results and the palaeoclimate estimates (Fig. 5). In addition, the temperatures estimated in this model might be too warm and/or too cool for some ages. The phase lags and some extremes shown in the results might be either because (1) some parts of this model are not appropriate, (2) input data may not represent a global average value or may have some errors (there is another possibility that some phase lags of Fig. 5 might be due to dif-

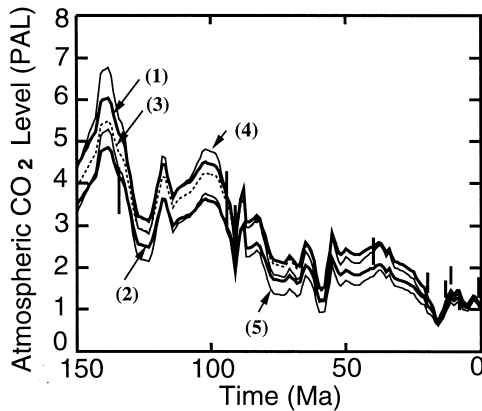


Fig. 6. The results of the temporal variation of the CO₂ level for various feedback functions used in the silicate weathering rate expression and also for the values of β : 1 = feedback function by Berner [6] with $\beta = 0.45$; 2 = feedback function by Berner with $\beta = 0.35$; 3 = feedback function by Walker et al. [8] with $\beta = 0.45$; 4 = feedback function by Volk [9] with $\beta = 0.35$; 5 = feedback function by Volk with $\beta = 0.25$.

ferences in the geological timescale used in different studies), and/or (3) there may be other dominant processes that control the atmospheric CO₂ budget and the climate at that time (for example, metamorphic CO₂ degassing from the Himalayan orogen and the Mediterranean Tethys and circum-Pacific orogenic belts in the early Cenozoic [39]). It is noted that CO₂ variation alone may not account for the climate change completely, because land elevation, land–sea distribution, vegetation, ocean circulation, ice albedo, and greenhouse gas species other than CO₂ will also affect the global climate in addition to the concentration of atmospheric CO₂ (e.g., [17,38,40–43]). Clearly, influences of all these factors should be considered in order to discuss the climate change in much more detail.

Fig. 6 shows the results for the cases with different weathering feedback functions. In order to obtain a consistent result with the biogeochemical estimates of palaeo-CO₂ levels [35], the value of β is estimated to be 0.35–0.45 when the feedback function by Berner [6] is used in the model. The results of the case for the feedback function by Walker et al. [8] are very similar to those of the case for Berner [6], although this agreement is considered to be something of a coincidence because Walker et al. [8] did not consider the biotic enhancement

of soil CO₂ levels. The result of CO₂ variation for the feedback function by Volk [9] is consistent with the biogeochemical estimates for palaeo-CO₂ levels when β is 0.25 to 0.35. This may be more preferable than the case of Berner [6] because the estimate of the global strontium budget suggests β to be ~ 0.25 [26], as described earlier. However, in this case, contrasts between high and low CO₂ levels seem to be somewhat large.

4. System analyses and discussion

In order to understand the climate change during this time, the results for the system analyses of the carbon cycle model are shown in Figs. 7–10. Figs. 7 and 8 show the results for the cases where specific forcing to the system are given. The case for $f_{SR} = f_h = f_D = f_{LA} = f_R = 1$ is defined here as the biological forcing case, because all these factors can be regarded as tectonic (mantle) forcing (in this case, the tectonic forcing is constant at the present value). Similarly, the case for $f_C = f_E = 1$, $\delta_{AO} = 1\%$, and $\Delta = 21.8\%$ is defined here as the tectonic forcing case, because all these factors can be regarded as a biological forcing (in this case, the biological forcing is constant at the present value). The results of these two cases are shown in Figs. 7 and 8. As shown in these figures, generally, the tectonic

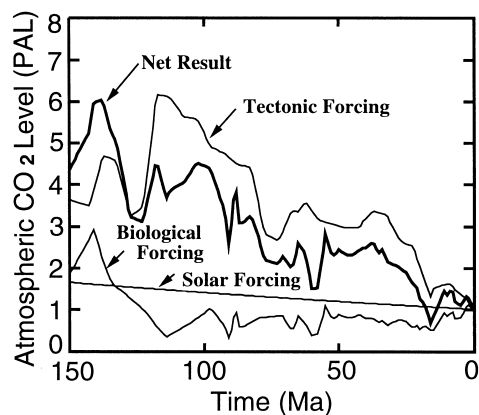


Fig. 7. The results of temporal variation of the CO₂ level by biological forcing ($f_{SR} = f_h = f_D = f_{LA} = f_R = 1$), tectonic forcing ($f_C = f_E = 1$, $\delta_{AO} = 1\%$, $\Delta = 21.8\%$) and solar forcing.

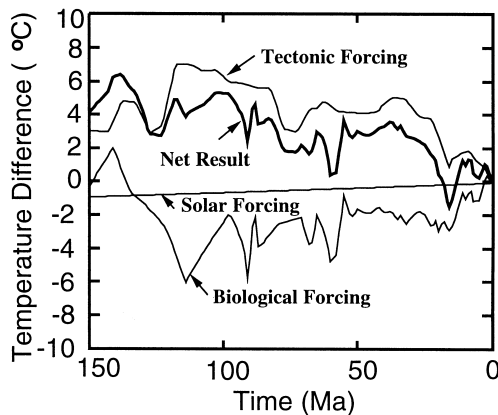


Fig. 8. The results of temporal variation of the global mean surface temperature for the cases of tectonic, biological, and solar forcing. Temperatures are shown as a difference from that of today ($= 15^{\circ}\text{C}$).

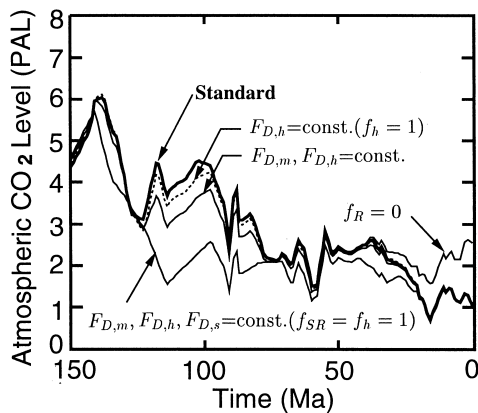


Fig. 9. The results of temporal variations of the CO_2 level for some tectonic forcings.

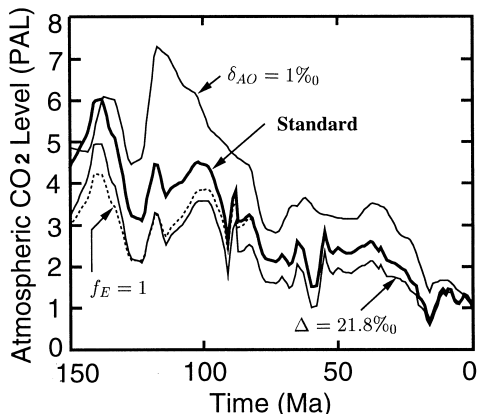


Fig. 10. The results of temporal variations of the CO_2 level for some biological forcings.

forcing results in warming, whereas the biological forcing results in cooling throughout the last 150 Ma. For example, between 100 Ma and 120 Ma, the biological forcing decreased the CO_2 level by 20–70% ($\Delta T \sim -1$ to -3°C) and the tectonic forcing increased it by 80–90% (ΔT 7.5–10 $^{\circ}\text{C}$) relative to the CO_2 level in the standard case (tectonic forcing + biological forcing). Therefore both these two forcings are equally important during this period. The net result, which takes into account both two forcings, is an intermediate, but the mid-Cretaceous is still very warm because of the strong effects of the tectonic forcing at that time. These results also suggest that the decrease in tectonic forcing may be responsible for the first-order cooling trend, and the biological forcing may be responsible for the second-order variations during this period. Figs. 7 and 8 show the solar forcing case where all factors except the solar luminosity are assumed to be constant at the present values. Although the change in solar luminosity is essential to the CO_2 level on the order of 10^9 years (e.g., [2,12–14,36]), its influence for the climate on this timescale ($\leq 10^8$ years) is very small (Figs. 7 and 8), because the solar luminosity was only 1.2% lower at 150 Ma than today. Fig. 9 shows the effects of tectonic forcing such as CO_2 degassing and the formation and uplift of the HTP. As expected from the magma eruption rates (Fig. 2), influences of mantle CO_2 degassing at mid-ocean ridges and hot spots are large during the mid-Cretaceous (see the case for $F_{D,m}$, $F_{D,h} = \text{constant}$). Between 120 Ma and 100 Ma, the 15–20% of CO_2 level is contributed by CO_2 degassing at mid-ocean ridges and hot spots (degassing of CO_2 due only to the eruption of oceanic plateau basalt at that time increases the CO_2 level by 5–10% for the same period). The enhanced total CO_2 degassing rate ($F_{D,m} + F_{D,h} + F_{D,s}^C + F_{D,s}^O$) due to the enhanced magma eruption and seafloor spreading rates contributes to the elevated atmospheric CO_2 level by 35–60% at that time (see the case for $F_{D,m}$, $F_{D,h}$, $F_{D,s}$ being constant). On the other hand, the CO_2 level decreased effectively after 40 Ma (about 150% of the present one) because of the enhanced erosion rate due to the formation and uplift of the HTP (see the case for $f_R = 0$). Similarly, Fig. 10 shows the results of the effects of biological forcing such as changes in soil biological activity and organic carbon burial rate. The case for $\delta_{AO} = 1\text{‰}$

results in an almost constant organic carbon burial rate throughout the last 150 Ma (within $\pm 10\%$ variations relative to the present-day value). In this case, as shown in Fig. 10, a generally higher CO_2 level and smoother variation than the standard case are obtained, suggesting that the CO_2 level, especially for the Cretaceous, tends to decrease (30–95% between 120 Ma and 100 Ma) owing to the enhanced organic carbon burial rate, and that the short-term variations of the CO_2 level, which may characterize the climate for each age (on a timescale of < 10 Ma), are caused by the short-term variations of the organic carbon burial rate during this period. It is noted that the resolution of the result depends largely on the resolution of the input data to the model, but correlation between the numerical results and the inferred palaeoclimates (Fig. 5) indicates the importance of the short-term variation of organic carbon burial rate for the short-term climate change. The increase in soil biological activity during the Cretaceous contributes to the decrease in the atmospheric CO_2 level (compare the case for $f_E = 1$ with the standard), which may also be a part of the reason for the general cooling trend. It is noted that the high CO_2 level around 140 Ma (150–130 Ma) is caused by the combination of the effects of tectonic forcing (especially of f_{SR} and f_h) and biological forcing (especially of $\delta^{13}\text{C}$ and f_E) as shown in Fig. 7. Although the exact timing for the largest effects of these factors is different (see Fig. 7), combination of these factors results in the high CO_2 level at that time. All these results suggest that the warm Cretaceous was the result of tectonic forcing such as the enhanced CO_2 degassing rate from the mantle and at subduction zones due to the increased mantle plume activity and seafloor spreading rates at that time, although the enhanced organic carbon burial could have had a tendency to decrease the CO_2 level effectively at that period. The cooling trend from the Cretaceous to the Cenozoic is caused mainly by tectonic forcing such as the decreasing CO_2 degassing rate and the enhanced erosion rate due to the formation and uplift of the HTP. However, the increase in soil biological activity is also a part of the causes for the cooling trend. The short-term variations of organic carbon burial rate seem to be responsible for the second-order variations of climate during the last 150 Ma.

5. Conclusions

The conclusions of this paper are summarized as follows:

(1) The variations of the atmospheric CO_2 level and of the global mean surface temperature during the last 150 Ma are reconstructed by using high-resolution data of crustal production rates of the mid-oceanic ridge basalt and oceanic plateau basalt, and of carbon isotopic composition of marine limestone. The model considered the enhanced volcanism and organic carbon burial rate, both of which may have characterized the carbon cycle during the Cretaceous. The silicate weathering process is formulated consistently with an abrupt increase in the marine Sr isotope record during the last 40 Ma.

(2) In addition to the first-order cooling trend, second-order variations of the atmospheric CO_2 level and the global mean surface temperature are also obtained. The results are in good agreement with previous estimates of the palaeo- CO_2 level and palaeoclimate from geological, biogeochemical, and palaeontological studies.

(3) The warm Cretaceous resulted from tectonic forcing such as the enhanced CO_2 degassing rate from the mantle, although the enhanced organic carbon burial may have decreased the CO_2 level at that time. The dominant controlling factors for the cooling trend of the climate during the last 150 Ma are tectonic forcing such as the decreasing volcanic activities, and the enhanced erosion rate due to the formation and uplift of the Himalayas and the Tibetan Plateau. In addition to these, biological forcing, such as the increase in soil biological activity due to the diversity of angiosperm–deciduous ecosystems, is also a part of the reason for the cooling trend.

(4) The short-term variations of the organic carbon burial rate seem to be responsible for the second-order variations of the climate. Such a variation of CO_2 may have characterized the climate for each epoch and age during the last 150 Ma.

Acknowledgements

I would like to thank R.A. Berner for his critical review and helpful comments. This research was partially supported by a grants-in-aid for Scientific

Research (No. 09740363) of the Ministry of Education of Japan. [RV]

References

- [1] L.A. Frakes, J.E. Francis, J.I. Syktus, *Climate Modes of the Phanerozoic*, Cambridge University Press, Cambridge, 1992, 274 pp.
- [2] J.F. Kasting, Theoretical constraints on oxygen and carbon dioxide concentrations in the Precambrian atmosphere, *Precambrian Res.* 34 (1987) 205–229.
- [3] R.A. Berner, A.C. Lasaga, R.M. Garrels, The carbonate–silicate geochemical cycle and its effect on atmospheric carbon dioxide over the past 100 million years, *Am. J. Sci.* 283 (1983) 641–683.
- [4] A.C. Lasaga, R.A. Berner, R.M. Garrels, An improved geochemical model of atmospheric CO₂ fluctuations over past 100 million years, in: E.T. Sundquist, W.S. Broecker (Eds.), *The Carbon Cycle and Atmospheric CO₂: Natural Variations Archean to Present*, American Geophysical Union, Washington, DC, 1985, pp. 397–411.
- [5] R.A. Berner, A model for atmospheric CO₂ over Phanerozoic time, *Am. J. Sci.* 291 (1991) 339–376.
- [6] R.A. Berner, GEOCARB II: a revised model of atmospheric CO₂ over Phanerozoic time, *Am. J. Sci.* 294 (1994) 56–91.
- [7] R.A. Berner, The rise of plants and their effect on weathering and atmospheric CO₂, *Science* 276 (1997) 544–546.
- [8] J.C.G. Walker, P.B. Hays, J.F. Kasting, A negative feedback mechanism for the long-term stabilization of Earth's surface temperature, *J. Geophys. Res.* 86 (1981) 9776–9782.
- [9] T. Volk, Feedbacks between weathering and atmospheric CO₂ over the last 100 million years, *Am. J. Sci.* 287 (1987) 763–779.
- [10] R.A. Berner, Biogeochemical cycles of carbon and sulphur and their effect on atmospheric oxygen over Phanerozoic time, *Palaeogeogr., Palaeoclimatol., Palaeoecol.* 75 (1989) 97–122.
- [11] K. Caldeira, M.R. Rampino, The mid-Cretaceous super plume, carbon dioxide, and global warming, *Geophys. Res. Lett.* 18 (1991) 987–990.
- [12] E. Tajika, T. Matsui, The evolution of the terrestrial environment, in: H.E. Newsom, J.H. Jones (Eds.), *Origin of the Earth*, Oxford Univ. Press, New York, NY, 1990, pp. 347–370.
- [13] E. Tajika, T. Matsui, Evolution of terrestrial proto-CO₂-atmosphere coupled with thermal history of the Earth, *Earth Planet. Sci. Lett.* 113 (1992) 251–266.
- [14] E. Tajika, T. Matsui, Degassing history and carbon cycle: from an impact-induced steam atmosphere to the present atmosphere, *Lithos* 30 (1993) 267–280.
- [15] J.F. Kasting, Comments on the BLAG model: the carbonate–silicate geochemical cycle and its effect on atmospheric carbon dioxide over the past 100 million years, *Am. J. Sci.* 284 (1984) 1175–1182.
- [16] R.A. Berner, E.J. Barron, Comments on the BLAG model: factors affecting atmospheric CO₂ and temperature over the past 100 million years, *Am. J. Sci.* 284 (1984) 1183–1192.
- [17] E.J. Barron, A warm, equable Cretaceous: the nature of the problem, *Earth Sci. Rev.* 18 (1983) 305–338.
- [18] W.C. Pitman, Relationship between eustasy and stratigraphic sequences of passive margins, *Geol. Soc. Am. Bull.* 89 (1978) 1289–1403.
- [19] R.L. Larson, Latest pulse of Earth: evidence for a mid-Cretaceous super plume, *Geology* 19 (1991) 547–550.
- [20] M.E. Raymo, W.F. Ruddiman, Tectonic forcing of late Cenozoic climate, *Nature* 359 (1992) 117–122.
- [21] M. Javoy, F. Pineau, C.J. Allègre, The carbon geodynamical cycle, *Nature* 300 (1982) 171–173.
- [22] J.C.G. Walker, Carbon geodynamic cycle, *Nature* 303 (1983) 730–731.
- [23] D.J. Des Marais, Carbon exchange between the mantle and crust, and its effect upon the atmosphere: today compared to Archean time, in: E.T. Sundquist, W.S. Broecker (Eds.), *The Carbon Cycle and Atmospheric CO₂: Natural Variations Archean to Present*, American Geophysical Union, Washington, DC, 1985, pp. 602–611.
- [24] M.A. Knoll, W.C. James, Effect of the advent and diversification of vascular land plants on mineral weathering through geologic time, *Geology* 15 (1987) 1099–1102.
- [25] M.E. Raymo, W.F. Ruddiman, P.N. Froelich, Influence of late Cenozoic mountain building on ocean geochemical cycles, *Geology* 16 (1988) 649–653.
- [26] F.M. Richter, D.B. Rowley, D.J. DePaolo, Sr isotope evolution of seawater: the role of tectonics, *Earth Planet. Sci. Lett.* 109 (1992) 11–23.
- [27] N. Harris, Significance of weathering Himalayan metasedimentary rocks and leucogranites for the Sr isotope evolution of seawater during the early Miocene, *Geology* 23 (1995) 795–798.
- [28] D.J. Des Marais, J.G. Moore, Carbon and its isotopes in mid-oceanic basaltic glasses, *Earth Planet. Sci. Lett.* 69 (1984) 43–57.
- [29] B. Marty, A. Jambon, C/³He in volatile fluxes from the solid Earth: Implications for carbon geodynamics, *Earth Planet. Sci. Lett.* 83 (1987) 16–26.
- [30] W.T. Holser, M. Schidlowski, F.T. Mackenzie, J.B. Maynard, Biogeochemical cycles of carbon and sulphur, in: C.B. Gregor, R.M. Garrels, F.T. Mackenzie, Maynard J.B. (Eds.), *Chemical Cycles in the Evolution of the Earth*, Wiley, New York, NY, 1988, pp. 105–174.
- [31] M.A. Arthur, W.E. Dean, G.E. Claypool, Anomalous ¹³C enrichment in modern marine organic carbon, *Nature* 315 (1985) 216–218.
- [32] N.J. Shackleton, M.A. Hall, Carbon isotope data from Leg 74 sediments, *Init. Rept. DSDP 74* (1984) 613–619.
- [33] N.J. Shackleton, The carbon isotope record of the Cenozoic: history of organic carbon burial and of oxygen in the ocean and atmosphere, in: J. Brooks, A.J. Fleet (Eds.), *Marine Petroleum Source Rocks*, *Geol. Soc. London Spec. Publ.* 26 (1987) 423–433.
- [34] M.A. Arthur, W.E. Dean, S.O. Schlanger, Variations in the global carbon cycle during the Cretaceous related to cli-

- mate, volcanism, and changes in atmospheric CO₂, in: E.T. Sundquist, W.S. Broecker (Eds.), *The Carbon Cycle and Atmospheric CO₂: Natural Variations Archean to Present*, American Geophysical Union, Washington, DC, 1985, pp. 504–529.
- [35] K.H. Freeman, J.M. Hays, Fractionation of carbon isotopes by phytoplankton and estimates of ancient CO₂ level, *Global Biogeochem. Cycles* 6 (1992) 185–198.
- [36] K. Caldeira, J.F. Kasting, The life span of the biosphere revisited, *Nature* 360 (1992) 721–723.
- [37] B.W. Sellwood, G.D. Price, P.J. Valdes, Cooler estimates of Cretaceous temperature, *Nature* 370 (1994) 453–455.
- [38] E. J. Barron, W.M. Washington, The role of geographic variables in explaining palaeoclimates: results from Cretaceous climate model sensitivity studies, *J. Geophys. Res.* 89 (1984) 1267–1279.
- [39] D.M. Kerrick, K. Caldeira, Metamorphic CO₂ degassing and early Cenozoic palaeoclimate, *GSA Today* 4 (1994) 61–65.
- [40] E.J. Barron, J.L. Sloan, C.G.A. Harrison, Potential significance of land–sea distribution and surface albedo variations as a climatic forcing factor; 180 M.Y. to the present, *Palaeogeogr., Palaeoclimatol., Palaeoecol.* 30 (1980) 17–40.
- [41] T.J. Crowley, D.A. Short, J.G. Mengel, G.R. North, Role of seasonality in the evolution of climate during the last 100 million years, *Science* 231 (1986) 579–584.
- [42] B.L. Otto-Bliesner, Tropical mountains and coal formation: a climate model study of the Westphalian (306 Ma), *Geophys. Res. Lett.* 20 (1993) 1947–1950.
- [43] B.L. Otto-Bliesner, G.R. Upchurch, Vegetation-induced warming of high-latitude regions during the late Cretaceous period, *Nature* 285 (1997) 804–807.
- [44] R.A. Berner, Models for carbon and sulphur cycles and atmospheric oxygen: application to Palaeozoic geologic history, *Am. J. Sci.* 287 (1987) 177–196.
- [45] M. Schidlowski, A 3,800-billion-year isotopic record of life from carbon in sedimentary rocks, *Nature* 333 (1988) 313–318.
- [46] P.L. Heller, D.L. Anderson, C.L. Angevine, Is the middle Cretaceous pulse of rapid sea-floor spreading real or necessary?, *Geology* 24 (1996) 491–494.